# UC Irvine
## UC Irvine Previously Published Works

**Title**

ELISE: A Reinforcement Learning Framework to Optimize the Slotframe Size of the TSCH Protocol in IoT Networks

**Permalink**

https://escholarship.org/uc/item/4sm232mw

**Journal**

IEEE Systems Journal, PP(99)

**ISSN**

1932-8184

**Authors**

Jurado-Lasso, F Fernando

Barzegaran, Mohammadreza

Jurado, JF

et al.

**Publication Date**

2024

**DOI**

10.1109/jsyst.2024.3371429

**Copyright Information**

Peer reviewed

# ELISE: A Reinforcement Learning Framework to Optimize the Slotframe Size of the TSCH Protocol in IoT Networks

F. Fernando Jurado-Lasso ⬡, *Member, IEEE*, Mohammadreza Barzegaran ⬡, *Member, IEEE*, J. F. Jurado ⬡, and Xenofon Fafoutis ⬡, *Senior Member, IEEE*

*Abstract*—The Internet of Things is shaping the next generation of cyber–physical systems to improve the future industry for smart cities. It has created novel and essential applications that require specific network performance to enhance the quality of services. Since network performance requirements are application-oriented, it is of paramount importance to provide tailored solutions that seamlessly manage the network resources and orchestrate the network to satisfy user requirements. In this article, we propose ELISE, a reinforcement learning (RL) framework to optimize the slotframe size of the time slotted channel hopping protocol in IIoT networks while considering the user requirements. We primarily address the problem of designing a framework that self-adapts to the optimal slotframe length that best suits the user's requirements. The framework takes care of all function-alities involved in the correct functioning of the network, while the RL agent instructs the framework with a set of actions to determine the optimal slotframe size each time the user require-ments change. We evaluate the performance of ELISE through extensive analysis based on simulations and experimental evalu-ations on a testbed to demonstrate the efficiency of the proposed approach in adapting network resources at runtime to satisfy user requirements.

*Index Terms*—Network management, wireless sensor networks (WSNs), industrial Internet of Things (IIoT), reinforcement learning (RL), time slotted channel hopping (TSCH).

## I. INTRODUCTION

THE world has witnessed a shift from traditional com-munication networks that interconnect computers through well-established standards to a pervasive network of networks that provides internet connectivity even to the smallest phys-ical objects. This evolved communication network, known as the Internet of Things (IoTs), is the enabling technology for Industry 4.0, where operational technology meets information technology. These cutting-edge technologies have created novel and essential applications for industrial operations, such as smart cities, intelligent energy management, and transportation.

At the hardware level, intelligent electronic devices embedded with computing, communication systems, sensors, and actuators realize such applications. This has led to the development of wireless sensor network (WSN) technology, which is flexible, cost-effective, and suitable for embedding into small objects. WSN find applications in various industrial domains [1], [2], [3], and their architecture is constrained by size, cost, and limited resources, such as computation capabilities, energy, memory, and communication bandwidth. Effective management of these resources is crucial to ensure optimal performance over an extended period.

Performance optimization in WSNs involves addressing var-ious network performance aspects, including power consump-tion, delay, and reliability. While reducing energy consumption through periodic radio chipset sleep cycles is essential [4], it is equally important to employ precise scheduling algo-rithms for coordination among neighboring nodes. The IEEE 802.15.4—time slotted channel hopping (TSCH) standard pro-vides functionalities for link scheduling in low-rate WSNs [5], [6], influencing network performance in multifaceted ways. The scheduling algorithm, known as the scheduler, generates cyclic schedules called *slotframes*, determining the physical channel for transmission at each time point. The schedule signif-icantly affects network performance. Redundant links improve reliability and latency but increase power consumption as re-ceiving nodes wake up their radios more frequently. Smaller slotframe sizes enhance network reliability and latency at the expense of higher power consumption, while larger slotframe sizes minimize power consumption but compromise reliabil-ity and latency. To meet application needs, the scheduling algorithm must consider user requirements, enabling a tai-lored schedule that is flexible, adaptable, and reliable, ac-commodating dynamic changes in the environment and user requirements.

TABLE I
SUMMARY OF RELATED WORKS

| Article | Year | Topic | | | UR | Major contribution(s) |
|---------|------|-------|---------|-----|-----|------------------------|
| | | TSCH | SDWSNs | RL | | |
| [11] | 2015 | ✓ | ✗ | ✗ | ✗ | Autonomous scheduler for TSCH without control overhead that does not rely on centralized or distributed entities. |
| [13] | 2017 | ✗ | ✓ | ✗ | ✓ | A decision-making approach to select the routing protocol that best suits the application requirements to get optimal performance using supervised learning. |
| [7] | 2020 | ✓ | ✓ | ✗ | ✗ | An SDN-based network architecture that provides support to mobile nodes using TSCH. Mobile nodes have one up- and downlink to every node in the network regardless of their position in the WSN. |
| [8] | 2020 | ✗ | ✓ | ✗ | ✗ | An SDN-based approach to pinpoint mobile nodes in WSN. The approach features a mobility detector and a k-means cluster algorithm to decouple static from mobile nodes. |
| [12] | 2020 | ✓ | ✗ | ✗ | ✗ | A low-latency distributed scheduling function to optimize the End-to-End delay, and reliability. |
| [9] | 2021 | ✗ | ✓ | ✓ | ✗ | A traffic monitoring framework for SDWSNs. They trained a double deep Q-network (DDQN) agent to achieve the optimal flow rule match-field policy. |
| [10] | 2021 | ✗ | ✓ | ✓ | ✗ | An RL approach to select the best routing path that improves the QoS of the SDWSN. |
| [16] | 2022 | ✓ | ✗ | ✗ | ✗ | PRIL-based approach to reduce the idle listening time in TSCH networks. It aims to address and solve the ACK losses problem. |
| [17] | 2022 | ✓ | ✗ | ✗ | ✗ | A dynamic TSCH scheduler for mobile IoT environment aiming to reduce collisions in shared cells, PLR , and control traffic. |
| [18] | 2023 | ✓ | ✗ | ✗ | ✗ | A proactive approach to mitigate extreme coexistence issues among multiple independent TSCH networks by introducing time deviations to reduce consecutive collisions. |
| [14] | 2023 | ✓ | ✗ | ✓ | ✓ | An RL approach to configure the parameters of the CSMA/CA of the TSCH protocol to achieve distinctive QoS. |
| ELISE | 2023 | ✓ | ✓ | ✓ | ✓ | An open-source framework that self-configures network resources in runtime to satisfy the dynamic user requirements for SDN-based IoT networks. |

In this article, we propose an open-source reinforcement learning (RL) framework named ELISE[1] to optimize the slotframe size of TSCH networks, considering dynamic changes in user requirements. We address the problem of designing a framework that self-adapts the slotframe size of the TSCH schedule to the optimal length that best suits a set of user requirements. ELISE guides the network through a set of actions to determine the optimal slotframe size whenever user requirements change.

The main contributions of this article are as follows.

1) We develop a novel open-source framework that enables centralized network resource management and runtime reconfiguration of WSNs.
2) We develop an RL solution that utilizes the ELISE framework to self-adapt the network's reliability, power efficiency, and delay based on user requirements.
3) We design a reward model based on a multiobjective cost function that facilitates the selection of the best network configuration to meet user requirements.
4) We evaluate the performance of ELISE through extensive analysis using simulations and experimental evaluations on a testbed.

The rest of this article is organized as follows. Section II presents an overview of the related work. Section III provides a technical background on key concepts in the framework. Section IV provides a detailed description of the framework components. Section V explains the design of the RL framework. Section VI presents the experimental layout, the approximation model, the training process, and the experimental evaluation. Finally, Section VII concludes this article.

## II. RELATED WORK

Table I presents a summary of the latest research works on related topics. It also provides information related to the year

of conception, whether the given article considers user requirements, and major contributions. Research works [7], [8] strive to improve the network performance using software-defined wireless sensor networks (SDWSNs). The centralized architecture of SDWSNs allows the control plane to build a global view of the network that permits it to make better decisions, in this case, to provide support for mobile sensor nodes. The research work in [7] used a static TSCH schedule with redundant links for mobile nodes to improve reliability, whereas [8] used a supervised learning approach to separate mobile from static nodes. The authors in [9], [10] oversaw the IoT network through the centralized controller, which enables the collection of observations to design, implement and train a learning agent to maximize the accumulative reward of actions taken. The work in [9] focused on monitoring the SDWSN traffic, at granularity levels to mitigate flow-table overflows, while [10] uses a learning agent to find the optimal forwarding paths for the SDWSN. The authors in [11], [12] aimed to improve the performance of TSCH networks. Research work [12] objective is to reduce the packet latency. This is achieved by dividing the slotframe into small chunks. Sensor nodes select the chunk to transmit based on their distance to the border router to minimize the latency. The work in [11], which has been previously introduced, is an autonomous scheduler with little overhead that provides high reliability. The article in [13] main objective is to select among a set of routing algorithms the best that suits the given user requirements. The selection of the routing algorithm is achieved using a supervised learning approach. The research work in [14] presents an RL approach to configure the carrier-sense multiple access/collision avoidance (CSMA/CA) parameters in a multi-hop TSCH network. The framework utilizes neural networks to converge to quality of service (QoS) satisfying configurations efficiently. For an in-depth review of TSCH networks, see [15].

Overall, these studies aim to enhance the QoS in network applications. Performance metrics, such as energy, delay, and reliability are considered, but there has been limited attention given to real user needs. It is crucial to provide a customized

This article has been accepted for inclusion in a future issue of this journal. Content is final as presented, with the exception of pagination.

JURADO-LASSO et al.: ELISE: AN RL FRAMEWORK TO OPTIMIZE THE SLOTFRAME SIZE OF THE TSCH PROTOCOL IN IOT NETWORKS 3

TABLE II
SUMMARY OF NOTATION

| Symbol | Description |
|---|---|
| $\mathcal{V}, \nu_i$ | Set of network nodes, network node $i$ |
| $\mathcal{E}, \epsilon_{i,j}$ | Set of network links, network link between nodes $i$ and $j$ |
| $\mathcal{R}, r_i$ | Set of routes, route for stream $i$ |
| $\mathcal{T}, \tau_i$ | Set of network streams, network stream $i$ |
| $\mathcal{H}$ | Function that returns the node rank |
| $F$ | Set of channel frequencies |
| $G(\mathcal{V}, \mathcal{E})$ | Network graph |
| $C, c_j, |c|$ | Slotframe, timeslot $j$, timeslot length |
| $\lambda$ | Last scheduled timeslot |
| $\mu$ | Maximum valid slotframe size |
| $\mathcal{G}_{\max}$ | Maximum penalty |
| $\tilde{P}, \tilde{D}, \tilde{R}$ | Normalized power consumption, delay, and reliability |
| $\alpha, \beta, \gamma$ | User requirement for energy, delay, and reliability |



Fig. 1. Example of a TSCH schedule for a six-nodes topology.

engineering solution that seamlessly manages network resources and orchestrates the network to meet the specific requirements of applications or users. However, as observed from the table, this aspect has not received significant focus. While the work presented in [13] takes user requirements into account in their proposed approach, their supervised learning method encounters challenges in predicting the optimal routing algorithm in dynamic environments, such as WSNs. Furthermore, they do not consider the MAC layer, which is responsible for the duty cycle of sensor nodes in state-of-the-art WSNs, directly impacting power consumption, delay, and reliability. In contrast, ELISE provides a holistic and flexible solution rooted in SDN principles and RL to optimize the TSCH schedule. ELISE's approach is designed explicitly to meet user requirements efficiently, addressing the limitations observed in other frameworks. This distinction highlights the efficiency and innovative approach of ELISE in fulfilling user-specific network optimization needs.

## III. BACKGROUND

In this section, we briefly introduce the network model and the core technologies used throughout this article: TSCH and SDWSN. We then discuss research works that have used these technologies to improve network performance. The summary of notation used throughout this article is presented in Table II.

### A. Network Model

We model the network as a directed graph $G(\mathcal{V}, \mathcal{E})$, where $\mathcal{V}$ is the set of nodes, and $\mathcal{E}$ is the set of physical links. A node $\nu_i \in \mathcal{V}$ is the sender and/or receiver of network traffic. The number of network nodes is denoted with $|\mathcal{V}|$. A link $\epsilon_{i,j} \in \mathcal{E}$ is a full-duplex link that connects the two nodes $\nu_i$ and $\nu_j$. since the links are bidirectional, the link $\epsilon_{i,j}$ is equivalent to $\epsilon_{j,i}$. The number of network links is denoted with $|\mathcal{E}|$.

The network traffic is modeled with the concept of streams (also called flows) that represents a data packet from one sender (talker) to one or multiple receivers (listeners). We denote the set of network streams as $\mathcal{T}$. A stream $\tau_i \in \mathcal{T}$ is characterized by the talker and the receiver. In ELISE, we limit the number of listeners for each stream to one, i.e., unicast communication. However, the model can be easily extended to support multicast streams by adding each sender–receiver pair as a stream.
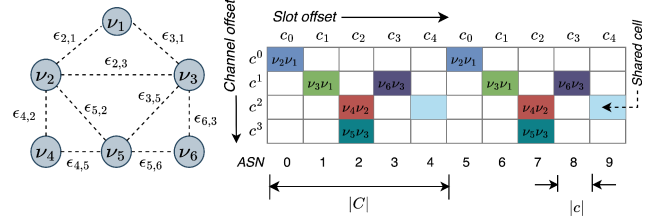
The path for the stream $\tau_i$ is determined as an ordered sequence of directed links and denoted with $r_i \in R$. Besides, $|r_i|$ represents the number of links in the path. For example, the stream $\tau_1 \in \mathcal{T}$ sending from the node $\nu_1$ to the node $\nu_3$ has the route $r_1 = \{\epsilon_{1,2}, \epsilon_{2,5}, \epsilon_{5,3}\}$. Using the set of routes $R$, we define the function $\mathcal{H} : \nu_i \longrightarrow \mathbb{N}$ which takes the node $\nu_i$ as the input and returns the node rank, i.e., the number of links originated for the node $\nu_i$, as the output. Fig. 1 presents an example of a TSCH schedule for six-node network topology.

### B. Software-Defined Wireless Sensor Networks

We model the network as an SDWSN. This architecture adopts concepts from software defined networking (SDN), which divides the control from the data functions, allowing the logically centralized controller to become reprogrammable and the WSN to be abstracted for applications and network services [19]. SDN separates the network into three network planes: application, control, and data plane. The application plane hosts applications and programs that send information about the network requirements to the SDN controller. In contrast, the control plane is a logically centralized entity that processes application requirements and sets up the network infrastructure resources to satisfy them. Finally, the data plane is the network infrastructure with little intelligence that follows orders from the control plane. Readers interested in a thorough background, challenges, and benefits of SDWSNs can refer to [19], [20], [21].

### C. Orchestra

Orchestra [11] is designed to run multiple stacked slotframes that repeat at different periods to ensure they do not interfere evenly. Each slotframe is allocated to a specific network plane that is defined by SDWSN. The scheduler selects the slotframe with higher priority to run when multiple slotframes need the communication medium simultaneously. In its default configuration, Orchestra runs three slotframes: 1) Enhanced Beacon (EB), 2) unicast, and 3) default traffic slotframes. The EB slotframe is a communication link from sensor nodes to its children to set the time source. The unicast slotframe contains links to every neighbor in the WSN. The default slotframe is used for traffic other than EB and unicast.

### D. Time Slotted Channel Hopping

TSCH is a globally synchronized network where traffic is transmitted based on a static cyclic schedule table called slotframe $C$ that repeats with the period equal to the slotframe

size $|C|$ [22], [23]. In a TSCH network, the slotframe (schedule) is divided into equal-length timeslots, as shown in Fig. 1. We denote each timeslot with $c_j \in C$ and its length with $|c|$ (same length for all timeslots). The timeslot length $|c|$, typically 10 ms, is long enough for the transmission and acknowledgment of frames.

To this end, the slotframe size $C$ is equal to the size of $n$ timeslots, denoted with $|C| = n \times |c|$. Within a slotframe, timeslots are counted with their subscripts $j$. Similarly, the timeslots can be counted from when the network booted with an absolute slot number (ASN). The ASN serves as a global clock, and it increases at every timeslot.

Each timeslot $c_j$ is divided into a fixed number of cells. Each cell denoted with $c_j^k$ indicates the channel offset $k$. For channel hopping a cell is used to find the physical channel to transmit. Considering an array of channel frequencies $F$ to hop over, the channel frequency $f$ for the cell $c_j^k$ is calculated in

$$f = F[(j + k)\%|F|]. \tag{1}$$

To this end, each cell will select a different physical channel at consecutive slotframes. The scheduler oversees the role of cells in the slotframe. The roles can be shared, dedicated, or empty cells. Shared cells (light blue cells in the example) are contention-based. They are used by multiple transmitters, increasing the probability of interference as they can transmit simultaneously. Reliable transmissions resend frames using a backoff window when no acknowledgment is received. Dedicated cells (cells labeled with a pair of nodes) are contention-free. They are allocated carefully not to cause interference issues with other cells. Retransmissions can occur due to external interference or bad radio link quality [12].

The example provides an illustration of a TSCH schedule that has been designed for a six-node WSN. The slotframe size is five timeslots $n = 5$. There are six cells with a nonempty role, one shared cell shown with $c_4^2$. There are five dedicated cells that permit the communication of nodes with their parents. There are also two noninterfering transmissions at the same slot offset $(c_2^2, c_2^3)$.

## IV. ELISE FRAMEWORK ARCHITECTURE OVERVIEW

This section presents an overview of the ELISE functional framework and architecture. Next, a detailed description of their components is presented, such as the layered architecture planes.

A high-level overview of the ELISE framework architectural structure, including its main components and interfaces, is shown in Fig. 2. The architectural structure follows the typical three-tier SDN principles for WSNs. The description of each layer of the architecture from the bottom-up is as follows.

### A. Data Plane

The data plane is built upon the interconnection of multiple wireless sensor nodes, for simplicity we call them sensors. In ELISE, we have defined two types of sensors: the (regular) sensor node and the sink. All sensor nodes, including the sink, communicate with each other using IEEE 802.15.4 radios; however, the sink is also directly connected to the control plane
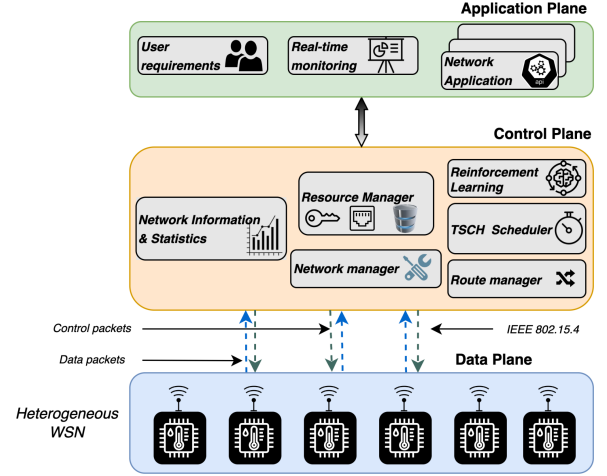


Fig. 2. ELISE architecture.

through a wired interface. All sensor nodes of the network graph that are denoted with $\nu \in \mathcal{V}$ and all radio communication links are denoted with $\epsilon \in \mathcal{E}$, see Section III-A for more information. Besides, we assume that sensor nodes are the talkers of network streams and all streams have the same listener node, i.e., the sink or the controller node.

Overall the entire network infrastructure runs on a lightweight embedded operating system. Among the available embedded operating systems in the market [19], we have selected Contiki-NG [24] because:

1) it is open-source, well documented, and it has a large community;
2) it is widely used in the research community;
3) it provides the implementation of TSCH and Orchestra;
4) it can run on both Cooja network simulator [25] and real hardware.

To align with SDWSN principles, we have re-engineered the protocol stack from layer three and above to support the following five functionalities. These functionalities utilize the forwarding packet depicted in Fig. 3(a), which includes fields for the protocol version, payload protocol, total packet length, header checksum, source and destination addresses.

*1) Neighbor Advertisement (NA):* This packet reports status and neighbor data to the controller, including the average power consumption, rank, and neighbor links. The packet header format is shown in Fig. 3(b). It includes the payload length field to specify the payload size, the sender's rank, sender's power consumption, cycle sequence, sequence fields (with the same function as in the data packet), and a CRC field for packet integrity checks. The payload contains neighbor addresses, received signal strength indicator (RSSI), and link quality indicator values.

*2) Network Configuration—TSCH Schedules:* This packet type is a control message for establishing the TSCH schedules in the upcoming cycle. The header, shown in Fig. 3(c), has four fields: payload length, slotframe size $|C|$, sequence, and CRC. The payload length, sequence, and CRC fields serve the same purposes as mentioned earlier. The slotframe size field indicates
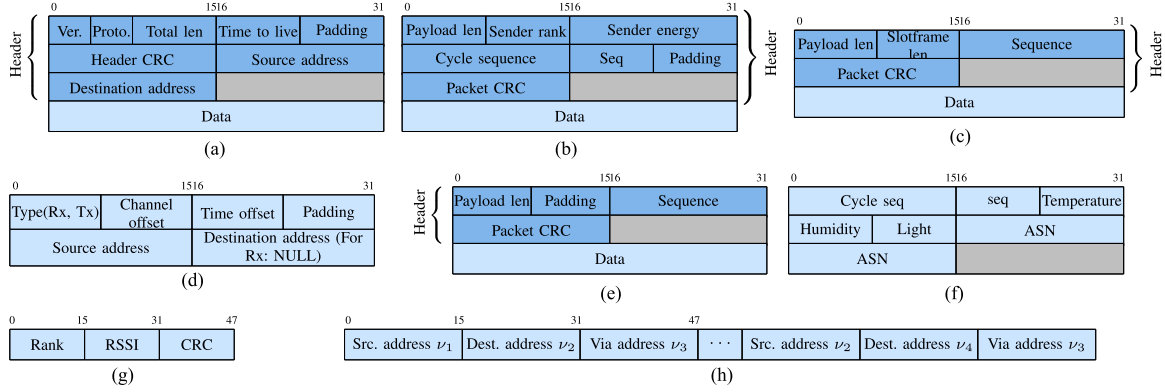
Fig. 3. Packet formats. (a) Forwarding packet format. (b) NA packet format. (c) TSCH packet format. (d) TSCH schedule payload format. (e) Route advertisement packet format. (f) Data packet format. (g) ND packet format. (h) Route advertisement payload format.

the schedule's length in the payload. The TSCH link format within this control packet's payload is in Fig. 3(d). The type field states the link type: transmit (Tx) or listen (Rx). The channel and time offset fields specify the link's coordinates. The source address indicates the sensor node requiring processing this link, and the destination address is used for Tx link types to set the neighbor address.

*3) Network Configuration—Routes:* This packet type is a control message to establish forwarding paths for the incoming cycle. The packet header, depicted in Fig. 3(e), includes payload length, sequence, and CRC fields serving the same function as mentioned earlier. The packet payload, depicted in Fig. 3(h), contains source, destination, and neighbor addresses for building the forwarding paths.

*4) Data Packets:* The packet format in Fig. 3(f) includes cycle sequence and sequence fields, used by the RL algorithm to track received packet counts in the corresponding cycle. It also has physical variables, such as temperature, humidity, and light (this can be generalized to variables one, two, and three). In addition, the ASN field contains a creation timestamp, useful to calculate the packet latency under specific network configurations, such as routes and TSCH schedules.

*5) Neighbor Discovery (ND):* This packet [see Fig. 3(g)] serves to discover other sensor devices within sender's transmission range, and identify neighbors with paths to the controller. It has three fields: rank (equivalent to $\mathcal{H}$), representing the number of links originating from the talker node as discussed in Section III-A; RSSI, indicating accumulative RSSI to the controller, helping receiver nodes in parent selection when rank values are equal; and a checksum field for error checking and packet integrity assurance.

Control packets, including TSCH schedules and route packets, are broadcast within the WSN. ELISE defines four slotframes, inspired by Orchestra, for specific traffic purposes: the EB slotframe for the time source, the control traffic slotframe for control packets, the data traffic slotframe for data packets, and the default traffic slotframe for other traffic types. The control traffic serves as a broadcast slotframe for transmitting and receiving new TSCH schedules and route configurations.

For cell $c_j^k$, the time slot number $j$ and channel offset $k$ for sensor node $\nu_i$ and control plane slotframe size of $|C|$ are calculated as follows:

$$j = \mathcal{H}(\nu_i)\%|C|$$
$$k = ((i)\%|C| - 1) + 1. \tag{2}$$

These two equations minimize communication interference between sensor nodes with equal rank values that try to broadcast control packets to their children.

### B. Control Plane

The control plane can run locally on a computer or in the cloud. At its core, it is implemented in Python 3 [26] because it supports multiple machine learning libraries available in the market, has a large community, and has an ample library collection. Here, we briefly introduce the core functionalities of each module.

*1) Network Information and Statistics:* This module holds all network information collected. It also includes all packets received and simple statistics.

*2) Resource Manager:* This module is in charge of orchestrating all resources in the control plane. Resources in this module include database, serial interface, and network access.

*3) Network Manager:* This module holds key functions to correctly operate the data plane. Functions such as writing and reading from the network reside here.

*4) Route Manager:* This module hosts all functionalities to build the forwarding paths of the network. It hosts multiple traditional routing algorithms. It is also flexible to allow adding new centralized routing protocols.

*5) TSCH Manager:* In this module resides the functions to correctly build TSCH schedules. It has been designed to easily create new TSCH schedulers on top.

*6) Reinforcement Learning:* The RL module is the main intelligent component of the entire control plane. It uses all other modules to collect data, learn from the environment, tune hyperparameters and evaluate the trained agent. This module is discussed in detail in the next section.
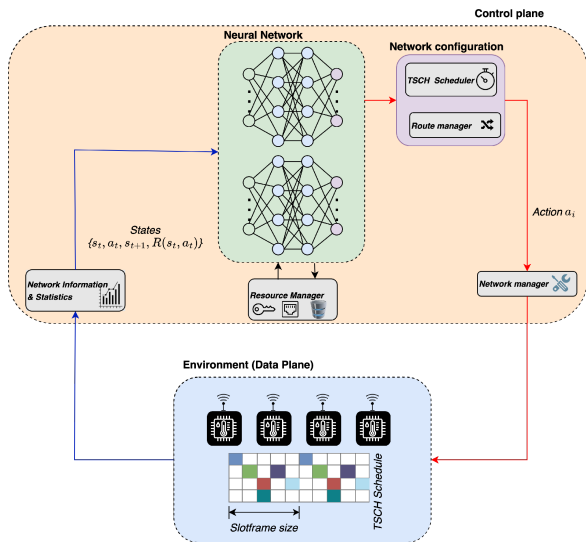
Fig. 4. Architecture of the RL agent of ELISE.

## C. Application Plane

The application plane hosts user requirements and programs, such as real-time monitoring tools that convey information regarding the status of the network. This plane instructs the control plane on the current user requirements through the northbound API.

## V. RL MODULE

This section takes the reader through the design and implementation of a RL approach to optimize the slotframe size of TSCH in SDN-based IoT networks considering the user requirements. Readers interested in RL can refer to [27] and its applications to SDWSNs in [19].

## A. Solution Approach

To solve this multiobjective function that self-adapts the slotframe size of the TSCH schedule to the optimal length that best suits a set of user requirements, we use an RL agent that hosts neural networks in its core, as shown in Fig. 4. ELISE provides flexibility to evaluate different RL algorithms. Algorithms that we consider in this research are deep Q network (DQN) [9], asynchronous advantage actor critic (A2C) [28], and proximal policy optimization (PPO) [29].

The proposed solution follows the typical three-tier principles for SDWSNs, where the control plane layer collects data, orchestrates resources, performs intelligent calculations, and deploys new network configurations into sensor nodes. At the initial state of the data plane, sensor nodes discover their path to the controller using ND packets. They then start sending NA packets to the controller. The controller processes these packets to make future decisions. The RL agent predicts the next slotframe size. It then prepares the TSCH schedules and routes using the TSCH and route manager module. Finally, the control plane deploys new configurations through the network management module.

ELISE develops a Markov decision process (MDP) framework with the architecture depicted in Fig. 4. This framework enables the RL algorithm to dynamically select and deploy optimal actions based on the observations to maximize the average accumulative reward. The MDP is represented by a tuple $< \mathcal{S}, \mathcal{A}, \mathcal{R} >$, where $\mathcal{S}$ represents the state space, $\mathcal{A}$ represents the action space, and $\mathcal{R}$ represents the immediate reward.

1) State space: As previously discussed, there are three performance metrics, and three user requirements, at the end of each iteration. However, the learning time can be reduced by adding the last scheduled link in the TSCH slotframe ($\lambda$), and the current slotframe size ($|C|$). $\lambda$ enables the agent to avoid slotframe sizes that are below the last scheduled link in the scheduler, otherwise, it can alter the normal behavior of the TSCH network. The state space of the proposed work is defined as follows:

$$\mathcal{S} \triangleq \{(\Omega_1, \alpha_1, \beta_1, \gamma_1, \lambda_1, |C|_1), \dots,$$
$$(\Omega_n, \alpha_n, \beta_n, \gamma_n, \lambda_n, |C|_n)\} \qquad (3)$$

where $\Omega$ represents the cost of the SDWSN. $\alpha$, $\beta$, and $\gamma$ are the user-defined coefficients for power consumption, delay, and reliability, respectively.

2) Action space: The RL agent aims to find the optimal slotframe size of the data plane traffic plane given the set of user requirements. At every decision-making point, the agent predicts the next slotframe size given the above-mentioned observations. The agent can take multiple consecutive actions (slotframe sizes) before reaching the optimal solution. The number of steps taken to reach the optimal solution depends on the current state of the environment, especially, the current slotframe size ($|C|$) and the user requirements ($\alpha$, $\beta$, $\gamma$).

The agent selects the next action between:
   a) increasing $|C|$;
   b) decreasing $|C|$; or
   c) continuing using the current $|C|$.

The selection of the slotframe size is bounded by numbers that are mutually prime to other slotframes in the TSCH network. Recall that the TSCH network runs multiple stacked slotframes that repeat at different periods (mutually prime slotframe sizes) to ensure they do not interfere evenly. Therefore, the action space for selecting the next slotframe size in the control plane is defined as follows:

$$\mathcal{A} \triangleq \{a : \gcd\left(a, |C|^{\text{EB}}, |C|^{\text{CP}}, |C|^{\text{DF}}\right) = 1\} \qquad (4)$$

where gcd represents the greatest common divisor, and $|C|^{\text{EB}}, |C|^{\text{CP}}$, and $|C|^{\text{DF}}$ are the slotframe sizes of the EB, control, and default traffic planes.

3) Immediate reward function: The reward function has been designed to select slotframe sizes within a valid range and to ease learning. Whenever the agent selects a slotframe size below $\lambda$, it is penalized. In the other case, whenever the agent selects a slotframe size that goes beyond the maximum valid slotframe size ($\mu$), it is also penalized. The agent learns to select the next action within this valid range while maximizing the accumulative reward. The

agent is positively rewarded if the slotframe size lies within the valid range. The amount rewarded depends on the performance metrics and user requirements. The reward function is expressed as follows:

$$\mathcal{R}(s,a) = \begin{cases} -\mathcal{G}_{\max}, & |C|^{\text{DP}} \geq \mu \\ & |C|^{\text{DP}} \leq \lambda \\ \Upsilon - \Omega, & \lambda < |C|^{\text{DP}} < \mu \end{cases} \quad (5)$$

where $|C|^{\text{DP}}$ is the slotframe size of the data traffic slotframe, and $\mathcal{G}_{\max}$ is the maximum penalty for taking an invalid slotframe size. $\Upsilon$ is a constant that makes sure the immediate reward stays always positive. $\Upsilon$ is equal to the worst case of $\Omega$. Therefore, $\Upsilon = 2$. We have defined two terminating conditions for episodes. We end an episode either every time the agent selects a slotframe size outside the valid range or when we reach the maximum number of timesteps.

### B. Optimization Problem

This RL-based model optimizes the slotframe size of the data plane slotframe introduced in the above-mentioned sections. Other slotframes are not considered in the optimization because they are control slotframes that are mandatory for the basic operation of the network, and tempering with them can make the network fail.

We formulate a weight-based multiobjective optimization problem that minimizes the cost of the TSCH schedule and the routing. This multiobjective optimization problem is formulated as follows:

$$\min_{|C|^{\text{DP}}} \Omega(|C|^{\text{DP}})$$

subject to $\alpha + \beta + \gamma = 1, \ \mathcal{T} > 0, \ |C|^{\text{DP}} \in \mathbb{N}$

$$\lambda < |C|^{\text{DP}} < \mu, \ \lambda > 0, \ |c| > 0$$

$$\gcd(|C|^{\text{DP}}, |C|^{\text{EB}}, |C|^{\text{CP}}, |C|^{\text{DF}}) = 1 \quad (6)$$

where $\Omega = \omega_1 \times \omega_2$, $\omega_1 = \alpha \times \widetilde{P} + \beta \times \widetilde{D} - \gamma \times \widetilde{R}$ captures the scheduling cost, and $\omega_2$ captures the routing cost. It is noteworthy that the negative sign in front of $\gamma$ is used because in this context, we aim at maximizing the reliability rather than minimizing it. Therefore, subtracting the reliability from the cost function helps to find the maximum reliability cases. The constraint $\alpha + \beta + \gamma = 1$ serves multiple crucial purposes.[2] First, it normalizes the weights, providing a consistent scale for comparing and interpreting results, thus facilitating a meaningful tradeoff analysis. Second, it empowers users to express their preferences and tailor the optimization process to their application requirements. Third, it enhances transparency by indicating that tradeoffs between objectives have been deliberately considered. This constraint aligns with mathematical

[2]Here, $\alpha$, $\beta$, and $\gamma$ represent user-defined weights that capture the relative importance of power consumption, delay, and reliability. The values of $\alpha$, $\beta$, and $\gamma$ are set by the user based on the specific application requirements. Interested readers can explore Pareto analysis for optimizing these weights.

foundations and simplifies the algorithmic implementation, providing a systematic, user-centric, and mathematically sound approach to objective prioritization. ELISE calculates performance metrics at the end of every cycle; therefore, the samples within the time interval are considered a constraint (they must be strictly greater than zero). This constraint applies to all performance metric samples. The slot duration in TSCH networks must be greater than zero. The optimization is performed over the slotframe size of the data plane slotframe in the TSCH protocol.

### C. Performance Metrics

The performance metrics are as follows: power consumption, delay, reliability, and dependability. The first three metrics are used in the cost term $\omega_1$ and the dependability is defined with $\omega_2$.

1) *Power Consumption:* In TSCH networks, nodes wake up their radios at specific timeslots to either transmit a packet or listen to the wireless medium, then switch to another state such as low power mode. In ELISE, we assume three states for a network node: a) listening, b) transmitting, c) listening and transmitting (forwarding). We ignore the idle state of the nodes since we aim at minimizing the workload of the network nodes.

The power consumed for transmitting the network stream $\tau_i \in \mathcal{T}$ from the talker to the listener denoted with $P_i$ is calculated from (7). The consumed power is normalized in the range [0,1]

$$P_i = \frac{\sum_{\epsilon_{m,n} \in r_i} (V^m \times I_{tx}^m + V^n \times I_{rx}^n) \times |c|}{(V^m \times I_{\max}^m + V^n \times I_{\max}^n) \times |C|} \quad (7)$$

where $V^i$ is the power supply voltage of the node $\nu_i$ (in volts), $I_{tx}^i$ is the transmission current consumption of the node $\nu_i$ and $I_{rx}^i$ is the reception current consumption of the node $\nu_i$ (both in mA). The maximum value of the current consumption while transmitting and receiving is captured by $I_{\max}$. The average power consumption of the network $\widetilde{P}$ is defined as the average of the power consumed for transmitting all network streams. The controller receives the NA packets from network nodes and processes the data in the sender power fields of the packets and stores them in the database. When a cycle finishes, the controller retrieves, from the database, the latest power consumption, and calculates the network power consumption cost $\overline{P}$ using

$$\widetilde{P}(\theta_1) = \bar{P} + \theta_1 \times \sigma_P, \ \bar{P} = \frac{1}{|\mathcal{T}|} \sum_{\tau_i \in T} P_i, \ \text{and}$$

$$\sigma_P = \sqrt{\frac{\sum_{\tau_i \in T} |P_i - \bar{P}|}{|\mathcal{T}|}} \quad (8)$$

where $\bar{P}$ is the average power consumption in the network, $\sigma_P$ is the normal distribution of the node power consumption in the network, and $\theta_1$ is the weight of the node power consumption distribution. The larger $\theta_1$ value drives the search for a solution with evenly distributed power consumption across the nodes. With $\theta_1$, the user achieves the desired distribution based on the requirements.

2) *Delay:* The packet delay is calculated as the interval from when the packet is generated at the talker to when the packet

is received by the listener in the control plane. For a TSCH network, we can estimate the packet delay of the stream $\tau_i$ as $D_i = (\text{ASN}_{tx} - \text{ASN}_{rx}) \times \frac{|c|}{|C|}$. The control plane then calculates the average delay of the network $\widetilde{D}$ using (9) at the end of each cycle. The controller retrieves from the database, the latest $\bar{D}$ for all network streams $\tau_i \in \mathcal{T}$

$$\widetilde{D}(\theta_2) = \bar{D} + \theta_2 \times \sigma_D, \ \bar{D} = \frac{1}{|\mathcal{T}|}\sum_{\tau_i \in T} D_i, \ \text{and}$$

$$\sigma_D = \sqrt{\frac{\sum_{\tau_i \in T}|D_i - \bar{D}|}{|\mathcal{T}|}} \qquad (9)$$

where $\sigma_D$ captures the normal distribution of stream delays. Using $\theta_2$ user can adjust the weight of delay distribution in calculating the average delay. The larger weight drives the search for a solution with evenly distributed stream delays. Similar to $\theta_1$, the user achieves the desired distribution using $\theta_2$ set.

*3) Reliability:* To calculate the reliability, we first define the packet delivery ratio (PDR) during a cycle. The control plane performs the calculation of the PDR ($\frac{|\tau_{rx}|}{|\tau_{tx}|}$, subject to $\tau_{tx} > 0$ where $\tau_{rx}$ and $\tau_{tx}$ are the numbers of received and transmitted packets, respectively). The control plane queries the database to obtain the latest PDR values in the network and calculates the network reliability $\widetilde{R}$ at every end of a cycle as follows:

$$\widetilde{R} = \frac{1}{|\mathcal{T}|}\sum_{\tau_i \in T} \text{PDR}_i \qquad (10)$$

where $\text{PDR}_i$ is the PDR of the stream $\tau_i \in \mathcal{T}$. The reliability of the network is calculated as the average of the reliability of all streams in the network.

*4) Dependability:* We define the dependability metric $\omega_2$ as the cost function for finding the best path for the streams in the network. The dependability metric is based on a simple concept, i.e., the network is more dependable where fewer nodes are involved in the network functioning (stream transmission). Based on this concept, the most dependable network is the one where all streams use the shortest path for transmission.

To this end, we define the power dependability PDEP of the node $\nu_i \in \mathcal{V}$ in (11). The power dependability of a node shows how much the node is under the workload, i.e., transmission and receiving the data. The more a node is under the workload, the less dependable is the node

$$\text{DEP}_i = \text{DEP}_i^{tx} + \text{DEP}_i^{rx}, \ \text{DEP}_i^{tx} = \sum(V^i \times I_{tx}^i \times |c|)$$

subject to $\forall \epsilon_{i,x} \in r_y$ and $\forall r_y \in R,$

$$\text{DEP}_i^{rx} = \sum(V^i \times I_{rx}^i \times |c|)$$

subject to $\forall \epsilon_{z,i} \in r_w$ and $\forall r_w \in R.$

$$\qquad\qquad (11)$$

The power dependability of the node represents the workload of the node, which is used for determining the most dependable path for a specific stream. Thus, we calculate the dependability of the stream $\tau_j \in \mathcal{T}$ as follows:

$$\text{DEP}_j = \prod \text{PDEP}_i, \ \text{subject to } \epsilon_{i,x} \in r_j. \qquad (12)$$
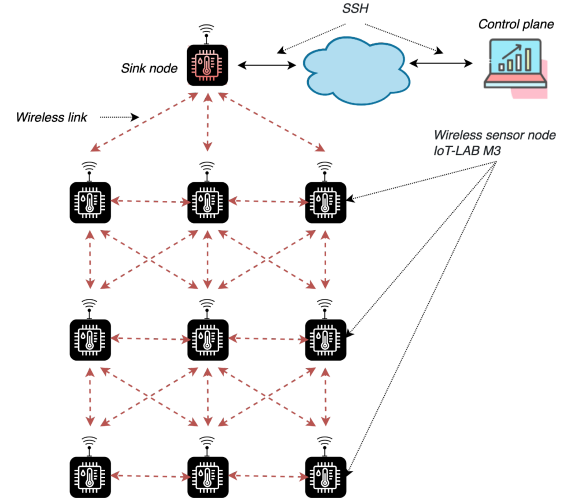


Fig. 5.　Topology of the testbed setup.

With the dependability of the streams in the network, we calculate the average dependability of the network $\omega_2$ using

$$\omega_2 = \frac{1}{|\mathcal{T}|}\sum_{\tau_j \in T} \text{DEP}_j, \ \text{subject to } |\mathcal{T}| > 0. \qquad (13)$$

## VI. PERFORMANCE EVALUATION

We compare ELISE's performance against Orchestra, the preferred TSCH scheduler for IoT networks. The experiments are conducted in both the Contiki Cooja network simulator and a real-world testbed. Due to space limitations, simulation results confirming the findings from the testbed experiments are omitted.

### A. Testbed Setup

The experiments were conducted at the FIT IoT Lab [30], using a ten-sensor-node network with a maximum depth of three hops. The topology is shown in Fig. 5. The network utilized the IoT-LAB M3 platform, consisting of ARM-Cortex M3 microcontrollers, ATMEL radios, and four sensors. The network run on Contiki-NG, with a redesigned network stack to support SDWSN functionalities. The control plane communicated with the data plane through the secure shell protocol and was implemented in Python 3.10 using Stable Baselines 3 [31] for RL. The experiment parameters are summarized in Table III. There exist a tradeoff between the iteration window interval. A large interval filters out noise but hampers dynamic changes, while a small interval increases noise and network reconfigurations. In our experiments we set this value to 60 control packets ($|\mathcal{T}| = 60$); however, this value can be changed to meet user requirements. Although with $\theta_1$ and $\theta_2$ in objective metrics (see Section V-C) the desired distribution of power and delay is achievable, for the evaluation where we have considered a fixed path for streams, we set both $\theta_1$ and $\theta_2$ to zero which remove the effect of power and delay distribution in the search. In future work, ELISE will determine the path for streams.

TABLE III
EXPERIMENT PARAMETERS

| Parameter | Value |
|---|---|
| No. of sensor nodes ($|\mathcal{V}|$) | 10 |
| Sensor nodes type | IoT-LAB M3 |
| Transmission power | $-17$dbm |
| Iteration window interval | 60pkts |
| Power measure sample time ($t_{sample}$) | 60s |
| Sensor node supply voltage ($V$) | 3V |
| Network node rank ($\mathcal{H}$) | 3 |
| TSCH slot duration ($|c|$) | 10ms |
| Reward constant $\Upsilon$ | 2 |
| Minimum slotframe size $\lambda$ | 10 |
| Maximum slotframe size $\mu$ | 70 |
| Penalty $\mathcal{G}_{max}$ | $-4$ |
| Max. episode length ($\mathcal{V}$) | 50 |
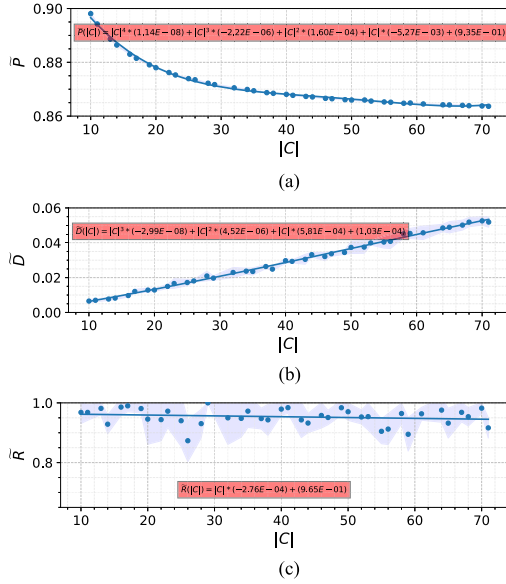


Fig. 6. Experimental $\widetilde{P}$ (a), $\widetilde{D}$ (b), and $\widetilde{R}$ (c) values for different slotframe sizes $|C|$.

## B. SDWSN Model Approximation

The SDWSN model approximation is used to estimate network performance metrics, such as average power consumption, average delay, and network reliability, based on the slotframe size in the TSCH network. This approximation model significantly reduces the iteration time required for training. The values of the performance metrics are estimated using the minimum mean square error estimator. The estimation is performed by sending TSCH schedules with different slotframe sizes and observing the resulting values. The estimated metrics are then used to calculate the immediate reward for actions taken. The approximation model is also used for hyperparameter tuning. The experimental setup and parameters are described, and the estimated values of the performance metrics against the slotframe size are plotted in Fig. 6. The results show that average power consumption decreases exponentially, while average delay increases linearly with the slotframe size. Network reliability decreases linearly but at a smaller rate. This approximation model
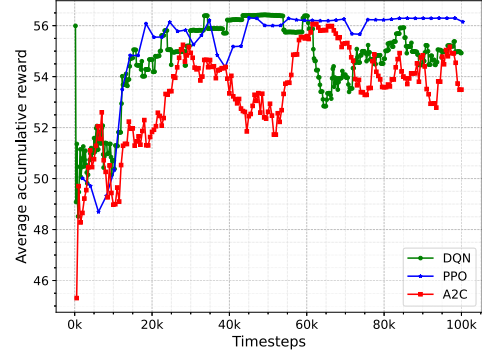


Fig. 7. Training of DQN, A2C, and PPO over 100 k iterations.

TABLE IV
EVALUATION OF DQN, A2C, AND PPO OVER 100 EPISODES

| Algorithm | Avg. accumulative reward |
|---|---|
| PPO | $56.44 \pm 0.11$ |
| A2C | $56.37 \pm 0.14$ |
| DQN | $56.34 \pm 0.15$ |

is used to train and test the DQN, A2C, and PPO algorithms in the testbed.

## C. Training

We train the agents over 100 k iterations, as illustrated in Fig. 7, which was completed $\approx$ 3 min using a 2.3 GHz 8-Core Intel Core i9 MacBook Pro with 16 GB of RAM. PPO seems to be the best candidate to solve the problem. However, we also evaluate the algorithms' performance by taking solely deterministic actions over 100 episodes to decide on which algorithm to pick. Table IV shows that PPO obtained the greatest average accumulative reward followed by A2C and DQN. Besides, Fig. 7 shows that PPO converges faster than A2C and DQN and depicts a more stable training process. Therefore, we use PPO for our result analysis in the testbed. We also tune the hyperparameters of the PPO model. For hyperparameter tuning, we used Optuna [32], which is a hyperparameter optimization framework for machine learning. We tune the hyperparameters for PPO using a random sampler and medium pruner, eight parallel jobs, with 1000 trials and a maximum of 50 000 steps.

## D. Experimental Evaluation

We evaluate the ELISE framework and the trained agent in the real-world testbed. The agent takes deterministic actions and is tested in a scenario with four distinct user requirements: balanced, prioritized delay, prioritized power consumption, and prioritized reliability. This scenario allows us to assess the agent's ability to select the best action based on observations and changing user requirements. The evaluation consists of ten episodes, each lasting for 160 iterations. Each iteration, representing the window interval, takes approximately 4 min. Therefore, each episode runs for around 10.6 hours. The initial slotframe size is set to 10 for all episodes. Results are plotted for each performance metric and the immediate reward against

This article has been accepted for inclusion in a future issue of this journal. Content is final as presented, with the exception of pagination.
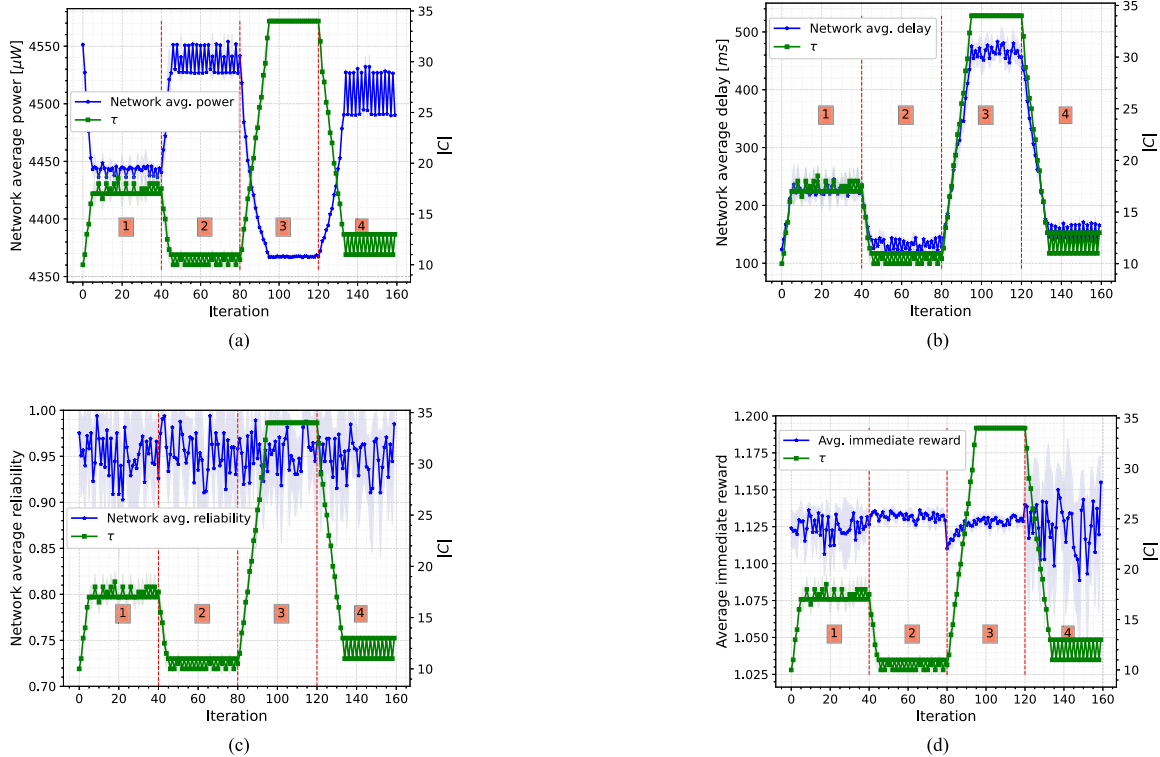


Fig. 8. Experimental evaluation of the ELISE framework and the RL agent for four user requirement cases. In zone 1, the balanced user requirements is running ($\alpha = 0.4$, $\beta = 0.3$, $\gamma = 0.3$). Zone 2 depicts the case for the prioritized delay user requirements ($\alpha = 0.1$, $\beta = 0.8$, $\gamma = 0.1$). Zone 3 shows the case for the prioritized power consumption user requirements ($\alpha = 0.8$, $\beta = 0.1$, $\gamma = 0.1$), and zone 4 represents the case for the prioritized reliability user requirements ($\alpha = 0.1$, $\beta = 0.1$, $\gamma = 0.8$). (a) Network average power consumption over the number of iterations. (b) Network average delay over the number of iterations. (c) Network average reliability over the number of iterations. (d) Network average immediate reward over the number of iterations.

the slotframe size using the 95% confidence interval. The experimental results are shown in Fig. 8.

*1) Balanced SDWSN:* Considering a balanced requirement where equal priority is given to all three performance metrics, we set the user coefficients $\alpha$, $\beta$, and $\gamma$ to 0.4, 0.3, and 0.3, respectively. This requirement is applied from timestep zero to timestep 40 (Zone 1 in Fig. 8). The trained agent takes an average of three actions to reach a steady state slotframe size ($|C|$) of 18, effectively balancing all performance metrics. The average power consumption is approximately 4443 $\mu$W [see Fig. 8(a)], the average delay is around 220 ms [see Fig. 8(b)], and the average reliability is about 0.95 [see Fig. 8(c)]. The network reliability exhibits a larger distribution due to interference sources in the testbed and the limited size of observations impacting reliability. The average immediate reward is approximately 1.13 [see Fig. 8(d)]. The dispersion in network reliability affects the reward distribution, although not to the same extent as in the prioritized reliability case.

*2) Prioritized Delay:* In this prioritized delay case, ELISE users assign higher priority to network delay compared to network reliability and power efficiency. The user coefficient values $\alpha$, $\beta$, and $\gamma$ are set to 0.1, 0.8, and 0.1, respectively. The prioritized delay requirement is activated after 40 timesteps and lasts for 40 timesteps (Zone 2 in Fig. 8). The RL agent promptly adjusts to the new requirements, reducing the slotframe size from an average of 18 to 11 in approximately three actions. Due to the emphasis on delay, the network average delay is

lower compared to other requirement cases. However, the network power consumption reaches its maximum as the slotframe size decreases. The network average delay, power consumption, and reliability are approximately 125 ms, 4540 $\mu$W, and 0.95, respectively [see Fig. 8(a)–(c)]. The average immediate reward is 1.13 and exhibits less variation compared to the previous case, reflecting the reduced contribution of network reliability in the reward function [see Fig. 8(d)].

*3) Prioritized Power Consumption:* For the prioritized power consumption case, the emphasis is on network power efficiency rather than network delay and reliability. The user coefficient values $\alpha$, $\beta$, and $\gamma$ are set to 0.8, 0.1, and 0.1, respectively. The requirements for this case are activated after 80 timesteps and last for 40 timesteps (Zone 3 in Fig. 8). The network transitions from a prioritized delay configuration to a prioritized power consumption configuration. The RL agent promptly detects the change in requirements (indicated by the immediate reward at timestep 80) and starts increasing the slotframe size. On average, the slotframe size increases from 11 to 34, taking around 13 actions to reach a steady state. As a result, the network experiences lower power consumption but higher delays overall. The network average delay, power consumption, and reliability are approximately 470 ms, 4367 $\mu$W, and 0.95, respectively [see Fig. 8(a)–(c)]. The average immediate reward is 1.14 and exhibits less variation compared to the balanced and reliable SDWSN cases, reflecting the reduced contribution of network reliability in the reward function [see Fig. 8(d)].

This article has been accepted for inclusion in a future issue of this journal. Content is final as presented, with the exception of pagination.

JURADO-LASSO et al.: ELISE: AN RL FRAMEWORK TO OPTIMIZE THE SLOTFRAME SIZE OF THE TSCH PROTOCOL IN IOT NETWORKS                11
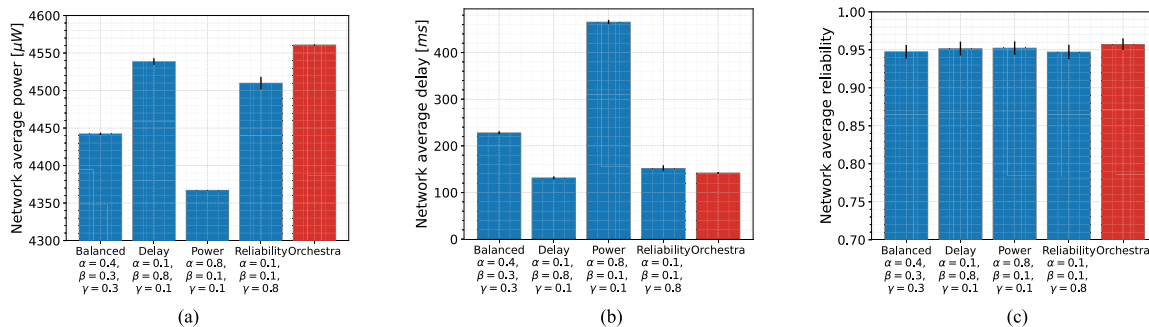
Fig. 9.     Experimental comparison between the ELISE framework and Orchestra. (a) Network average power consumption. (b) Network average delay. (c) Network average reliability.

*4) Prioritized Reliability:* For the prioritized reliability case, the focus is on network reliability rather than network power consumption and delay. The weights selected for this case are $\alpha = 0.1$, $\beta = 0.1$, and $\gamma = 0.8$. The requirements are applied at timestep 120 and last for 40 timesteps (Zone 4 in Fig. 8). At this point, the network transitions from a prioritized power consumption configuration to a prioritized reliability configuration. The RL agent detects the change in requirements and starts reducing the slotframe size. On average, it takes around 13 actions for the slotframe size to decrease to 12 and reach a steady state. Consequently, the network exhibits low delay [145 ms in Fig. 8(b)] and high power consumption [4510 $\mu$W in Fig. 8(a)]. The network reliability remains high with an average steady-state value of 0.95 [see Fig. 8(c)]. Overall, the network reliability is high for all user requirement cases, although it exhibits significant variation. This variation can be attributed to the frequency of TSCH schedule updates and the presence of multiple experiments and platforms in the densely populated testbed. The distribution of network reliability also impacts the immediate reward, but the RL agent successfully selects appropriate actions despite the noise [see Fig. 8(d)].

*5) ELISE and Orchestra:* Fig. 9 compares the ELISE framework with Orchestra in terms of network power consumption, delay, and reliability. ELISE adapts the slotframe size to optimize power consumption, resulting in lower average power consumption compared to Orchestra. ELISE also achieves smaller average delays, while Orchestra's delay is similar to the prioritized delay scenario. In terms of network reliability, Orchestra performs slightly better than ELISE, likely due to its autonomous scheduling and fewer control packets transmitted.

### E. Scalability

ELISE's scalability is underpinned by its machine learning-based approach, specifically a regression model. This model, founded on equations of multiple degrees, requires primarily constant updates as the network scales, ensuring its core structure remains stable. This consistency results in a relatively steady training time, simplifying the scalability process. However, the critical factor in ELISE's scalability is the availability of data. Like many other machine learning approaches, the ability to scale is often subject to the quality and quantity of the data. ELISE's architecture promotes scalability by facilitating the collection of comprehensive and representative data across diverse network sizes and scenarios.

### VII. Conclusion and Future Work

We introduced ELISE, an open-source framework that utilizes deep RL to optimize the slotframe size of TSCH for SDN-based IoT networks. ELISE effectively adapts network resources to dynamic user requirements and demonstrates its ability to maximize network performance. The framework encompasses various modules, including network management, data collection, schedule processing, route processing, and machine learning. Through experiments with different user requirements, ELISE showcases its ability to detect and respond to changes, achieving optimal performance. However, the evaluation process reveals challenges in real-world deployments, such as the time-consuming training phase and occasional packet loss during network reconfigurations. To address these issues, future work will focus on improving training efficiency and minimizing reliability impacts. The ultimate goal is to develop an autonomous RL scheduler within the ELISE framework that can adapt to user requirements seamlessly.

### Acknowledgment

### References

[1]  F. Deng, X. Yue, X. Fan, S. Guan, Y. Xu, and J. Chen, "Multisource energy harvesting system for a wireless sensor network node in the field environment," *IEEE Internet Things J.*, vol. 6, no. 1, pp. 918–927, Feb. 2019.

[2]  L. M. Borges, F. J. Velez, and A. S. Lebres, "Survey on the characterization and classification of wireless sensor network applications," *IEEE Commun. Surv. Tut.*, vol. 16, no. 4, pp. 1860–1890, Oct.–Dec., 2014.

[3]  G. P. Joshi, S. Y. Nam, and S. W. Kim, "Cognitive radio wireless sensor networks: Applications, challenges and research trends," *Sensors*, vol. 13, no. 9, pp. 11196–11228, 2013.

[4]  S. M. Chowdhury and A. Hossain, "Different energy saving schemes in wireless sensor networks: A survey," *Wireless Pers. Commun.*, vol. 114, no. 3, pp. 2043–2062, 2020.

[5]  D. Dujovne, T. Watteyne, X. Vilajosana, and P. Thubert, "6TiSCH: Deterministic IP-enabled industrial internet of things," *IEEE Commun. Mag.*, vol. 52, no. 12, pp. 36–41, Dec. 2014.

[6]  Y. Ha and S.-H. Chung, "Traffic-aware 6TiSCH routing method for IIoT wireless networks," *IEEE Internet Things J.*, vol. 9, no. 22, pp. 22709–22722, Nov. 2022.

[7] L. L. Bello, A. Lombardo, S. Milardo, G. Patti, and M. Reno, "Experimental assessments and analysis of an SDN framework to integrate mobility management in industrial wireless sensor networks," *IEEE Trans. Ind. Informat.*, vol. 16, no. 8, pp. 5586–5595, Aug. 2020.

[8] T. Theodorou and L. Mamatas, "SD-MIoT: A software-defined networking solution for mobile Internet of Things," *IEEE Internet Things J.*, vol. 8, no. 6, pp. 4604–4617, Mar. 2021.

[9] T. G. Nguyen, T. V. Phan, D. T. Hoang, T. N. Nguyen, and C. So-In, "Federated deep reinforcement learning for traffic monitoring in SDN-based IoT networks," *IEEE Trans. Cogn. Commun. Netw.*, vol. 7, no. 4, pp. 1048–1065, Dec. 2021.

[10] M. U. Younus, M. K. Khan, and A. R. Bhatti, "Improving the software-defined wireless sensor networks routing performance using reinforcement learning," *IEEE Internet Things J.*, vol. 9, no. 5, pp. 3495–3508, Mar. 2022.

[11] S. Duquennoy, B. Al Nahas, O. Landsiedel, and T. Watteyne, "Orchestra: Robust mesh networks through autonomously scheduled tsch," in *Proc. 13th ACM Conf. Embedded Netw. Sensor Syst*, 2015, pp. 337–350.

[12] V. Kotsiou, G. Z. Papadopoulos, P. Chatzimisios, and F. Theoleyre, "LDSF: Low-latency distributed scheduling function for industrial Internet of Things," *IEEE Internet Things J.*, vol. 7, no. 9, pp. 8688–8699, Sep. 2020.

[13] S. Misra, S. Bera, M. Achuthananda, S. K. Pal, and M. S. Obaidat, "Situation-aware protocol switching in software-defined wireless sensor network systems," *IEEE Syst. J.*, vol. 12, no. 3, pp. 2353–2360, Sep. 2018.

[14] H. Hajizadeh, M. Nabi, and K. Goossens, "Decentralized configuration of TSCH-BASED IoT networks for distinctive QoS: A deep reinforcement learning approach," *IEEE Internet Things J*, vol. 10, no. 19, pp. 16869–16880, Oct. 2023.

[15] A. Tabouche, B. Djamaa, and M. R. Senouci, "Traffic-aware reliable scheduling in TSCH networks for industry 4.0: A systematic mapping review," *IEEE Commun. Surv. Tuts*, vol. 25, no. 4, pp. 2834–2861, Oct.–Dec., 2023.

[16] S. Scanzio, G. Cena, and A. Valenzano, "Enhanced energy-saving mechanisms in TSCH networks for the IIoT: The PRIL approach," *IEEE Trans. Ind. Informat*, vol. 19, no. 6, pp. 7445–7455, Jun. 2023.

[17] W. Jerbi, O. Cheickhrouhou, A. Guermazi, and H. Trabelsi, "MSU-TSCH: A mobile scheduling updated algorithm for TSCH in the Internet of Things," *IEEE Trans. Ind. Informat.*, vol. 19, no. 7, pp. 7978–7985, Jul. 2023.

[18] M. Nabi, M. Habibollahi, and H. Saidi, "Time hopping: An efficient technique for reliable coexistence of TSCH-based IoT networks," *IEEE Internet Things J*, vol. 10, no. 15, pp. 13837–13848, Aug. 2023.

[19] F. F. Jurado-Lasso, L. Marchegiani, J. Jurado, A. M. Abu-Mahfouz, and X. Fafoutis, "A survey on machine learning software-defined wireless sensor networks (ML-SDWSNs): Current status and major challenges," *IEEE Access*, vol. 10, pp. 23560–23592, 2022.

[20] S. Bera, S. Misra, and A. V. Vasilakos, "Software-defined networking for Internet of Things: A survey," *IEEE Internet Things J.*, vol. 4, no. 6, pp. 1994–2008, Dec. 2017.

[21] H. I. Kobo, A. M. Abu-Mahfouz, and G. P. Hancke, "A survey on software-defined wireless sensor networks: Challenges and design requirements," *IEEE Access*, vol. 5, pp. 1872–1899, 2017.

[22] M. R. Palattella, N. Accettura, L. A. Grieco, G. Boggia, M. Dohler, and T. Engel, "On optimal scheduling in duty-cycled industrial IoT applications using IEEE802. 15.4 e TSCH," *IEEE Sensors J.*, vol. 13, no. 10, pp. 3655–3666, Oct. 2013.

[23] T. Watteyne, M. Palattella, and L. Grieco, "Using IEEE 802.15. 4e time-slotted channel hopping (TSCH) in the Internet of Things (IoT): Problem statement," Tech. Rep. rfc7554, 2015.

[24] G. Oikonomou, S. Duquennoy, A. Elsts, J. Eriksson, Y. Tanaka, and N. Tsiftes, "The Contiki-NG open source operating system for next generation IoT devices," *SoftwareX*, vol. 18, 2022, Art. no. 101089.

[25] F. Osterlind, A. Dunkels, J. Eriksson, N. Finne, and T. Voigt, "Cross-level sensor network simulation with COOJA," in *Proc. IEEE 31st Local Comput. Netw.*, 2006, pp. 641–648.

[26] M. Pilgrim and S. Willison, *Dive Into Python 3*, vol. 2. Berlin, Germany: Springer, 2009.

[27] N. C. Luong et al., "Applications of deep reinforcement learning in communications and networking: A survey," *IEEE Commun. Surv. Tut.*, vol. 21, no. 4, pp. 3133–3174, Oct.–Dec., 2019.

[28] V. Mnih et al., "Asynchronous methods for deep reinforcement learning," in *Proc. 33rd Int. Conf. Mach. Learn.*, 2016, pp. 1928–1937.

[29] J. Schulman, F. Wolski, P. Dhariwal, A. Radford, and O. Klimov, "Proximal policy optimization algorithms," 2017, *arXiv:1707.06347*.

[30] C. Adjih et al., "Fit IoT-lab: A large scale open experimental IoT testbed," in *Proc. IEEE 2nd World Forum Internet Things*, 2015, pp. 459–464.

[31] A. Raffin, A. Hill, A. Gleave, A. Kanervisto, M. Ernestus, and N. Dormann, "Stable-baselines3: Reliable reinforcement learning implementations," *J. Mach. Learn. Res.*, vol. 22, no. 1, pp. 12348–12355, 2021.

[32] T. Akiba, S. Sano, T. Yanase, T. Ohta, and M. Koyama, "Optuna: A next-generation hyperparameter optimization framework," in *Proc. 25th ACM SIGKDD Int. Conf. Knowl. Discov. Data Mining*, 2019, pp. 2623–2631.

**F. Fernando Jurado-Lasso** (Member, IEEE) received the B.Eng. degree in electronics engineering from the Universidad del Valle, Cali, Colombia, in 2012, and the M.Eng. degree in telecommunications engineering and the Ph.D. degree in engineering from The University of Melbourne, Melbourne, VIC, Australia, in 2015 and 2020, respectively.

He is currently a Postdoctoral Researcher with the Embedded Systems Engineering section of the Department of Applied Mathematics and Computer Science, Technical University of Denmark (DTU Compute), Lyngby, Denmark. His research interests include networked embedded systems, software-defined wireless sensor networks, machine learning, protocols and applications for the Internet of Things.



**Mohammadreza Barzegaran** (Member, IEEE) received the Ph.D. degree in computer science from the Technical University of Denmark, Lyngby, Denmark, in 2021.

Since 2023, he has been a Postdoctoral Research Fellow with the Center for Pervasive Communications and Computing, University of California, Irvine, Irvine, CA, USA. His research focuses on the configuration of fog computing platforms and wireless sensor networks. His research interests include wired and wireless sensor networks, fog/edge computing, real-time and critical systems.



**J. F. Jurado** received the B.Sc. degree from the Universidad de Nariño, Pasto, Colombia, in 1984, and the M.Sc. and Ph.D. degrees from the Universidad del Valle, Cali, Colombia, in 1986 and 2000, respectively, all in physics.

He is currently a Professor with the Faculty of Engineering and Administration, Department of Basic Science, Universidad Nacional de Colombia Sede Palmira, Palmira, Colombia. His research interests include nanomaterials, magnetic and ionic materials, nanoelectronics, embedded systems, and the Internet of Things.

Dr. Jurado is a Senior Member of Minciencias in Colombia.



**Xenofon Fafoutis** (Senior Member, IEEE) received the B.Sc. degree in informatics and telecommunications from the University of Athens, Zografou, Greece, in 2007, the M.Sc. degree in computer science from the University of Crete, Heraklion, Greece, in 2010, and the Ph.D. degree in embedded systems engineering from the Technical University of Denmark, Lyngby, Denmark, in 2014.

He is currently an Associate Professor with the Embedded Systems Engineering section of the Department of Applied Mathematics and Computer Science, Technical University of Denmark. His research interests include wireless embedded systems as an enabling technology for digital health, smart cities, and the (industrial) Internet of Things.